Macromolecular Bioscience
www.mbs-journal.de

In Vitro Evaluation of Anti-Aggregation and Degradation Behavior of PEGylated Polymeric Nanogels under In Vivo Like Conditions

Yinan Chen, George R. Dakwar, Kevin Braeckmans, Twan Lammers, Wim E. Hennink, and Josbert M. Metselaar**

The in vivo stability and biodegradability of nanocarriers crucially determine therapeutic efficacy as well as safety when used for drug delivery. This study aims to evaluate optimized in vitro techniques predictive for in vivo nanocarrier behavior. Polymeric biodegradable nanogels based on hydroxyethyl methacrylamide-oligoglycolates-derivatized poly(hydroxyethyl methacrylamide-co-*N*-(2-azidoethyl)methacrylamide) and with various degrees of PEGylation and crosslinking densities are prepared. Three techniques are chosen and refined for specific in vitro evaluation of the nanocarrier performance: (1) fluorescence single particle tracking (fSPT) to study the stability of nanogels in human plasma, (2) tangential flow filtration (TFF) to study the degradation and filtration of nanogel degradation products, and (3) fluorescence fluctuation spectroscopy (FFS) to evaluate and compare the degradation behavior of nanogels in buffer and plasma. fSPT results demonstrate that nanogels with highest PEGylation content show the least aggregation. The TFF results reveal that nanogels with higher crosslink density have slower degradation and removal by filtration. FFS results indicate a similar degradation behavior in human plasma as compared to that in phosphate buffered saline. In conclusion, three methods can be used to compare and select the optimal nanogel composition, and these methods hold potential to predict the in vivo performance of nanocarriers.

Dr. Y. Chen, Prof. T. Lammers, Prof. W. E. Hennink
Department of Pharmaceutics
Utrecht Institute for Pharmaceutical Sciences
Utrecht University
3584 CG, Utrecht, The Netherlands
E-mail: w.e.hennink@uu.nl
Dr. G. R. Dakwar, Prof. K. Braeckmans
Laboratory for General Biochemistry and Physical Pharmacy
Faculty of Pharmaceutical Sciences
Ghent University
9000 Ghent, Belgium
Prof. T. Lammers, Dr. J. M. Metselaar
Department of Nanomedicine and Theranostics
Institute for Experimental Molecular Imaging
RWTH Aachen University Clinic
52074 Aachen, Germany
Prof. T. Lammers, Dr. J. M. Metselaar
Department of Targeted Therapeutics
MIRA Institute for Biomedical Engineering and Technical Medicine
University of Twente
7522 NB, Enschede, The Netherlands
E-mail: bart@enceladus.nl

DOI: 10.1002/mabi.201700127

1. Introduction

Nanomedicines for intravenous administration have been extensively researched and developed with expected advantages: improvement of solubility and stability of drugs, generating more favorable pharmacokinetic and biodistribution behavior and achieving controlled drug release. These unique properties result in significant improvements in the efficacy and safety of the drugs.[1–4] A key feature to realize these advantages is a high stability and a controlled degradation behavior of the drug delivery system in vivo. Various in vitro characterization methods have been established with the aim to evaluate and optimize the stability and degradation behavior. However, those strategies often appear of limited value in the prediction of in vivo performance.[5] For instance, even though many colloidal drug carriers have shown high stability in buffer solution in vitro, they still easily aggregate in the in vivo situation, which is likely a consequence of proteins and cells in the biological fluids interacting with nanocarriers. This aggregation in turn further leads to rapid clearance of nanocarriers and poor therapeutic efficacy.[6–8] Modification of the particles with poly(ethylene glycol) (PEG) on the surface is a frequently applied method to decrease protein interaction and increase their stability in biological fluids.[9,10] Reduction of protein adsorption in the circulation can also decrease recognition and clearance by the mononuclear phagocyte system in the liver and spleen.[11,12] PEG molecular weight and PEG surface density are two major factors that determine in vivo performance. Thicker PEG layers that are formed with longer and denser PEG chains on the surface of particles normally lead to better shielding.[11,13] The effect of the degree of PEGylation on in vivo performance of nanomedicines is usually evaluated by studying pharmacokinetics and biodistribution in animals. Although it may be a straightforward approach, animal studies entail ethical issues and are time and cost consuming. There is thus an urgent need for better and more predictive in vitro characterization techniques that enable formulation optimization before in vivo experiments.

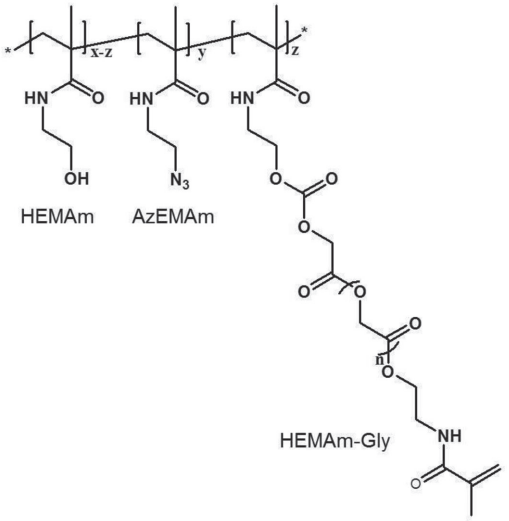

n = 0-3, average 0.83

DS*	AzEMAm%	(x-z)/y/z
5	5%	90/5/5
	10%	85/10/5
	20%	75/20/5
10	5%	85/5/10
	10%	80/10/10
	20%	70/20/10
20	5%	75/5/20
	10%	70/10/20
	20%	60/20/20

*DS: degree substitution of HEMAm-Gly

Figure 1. Chemical structures of p(HEMAm-co-AzEMAm)-Gly-HEMAm used in this manuscript with various contents of AzEMAm and different degrees of substitution.

Injected nanocarriers may result in potential toxicity and hazard healthy tissues in the body and biocompatibility and biodegradability are therefore crucial for nanocarriers.[14] Besides, the degradation behavior of drug-loaded nanocarriers can also alter the release and consequently the biodistribution of payloads.[15] Therefore, optimization of the degradation behavior of drug delivery system should be investigated to fulfill different requirements for various biomedical purposes. Several in vitro characterization techniques have been investigated to evaluate the degradation behavior of nanocarriers. A common method is to measure their weight loss during incubation.[16,17] Determination of changes in particle size as well as particle concentration in the suspension has also been investigated.[18,19] Assaying the degradation products is another way to study the degradation kinetics of nanoparticles.[19–21] However, while these techniques can provide important information about the physicochemical characteristics of the material used, they have limited predictive value for their in vivo performance as nanocarrier drug formulations.

This paper reports on three techniques that were specifically adopted and optimized to more accurately investigate and predict in vivo performance of nanocarrier formulations. Nanogels are nanosized hydrogel particles consisting of water-swollen hydrophilic polymeric networks. They possess combined attractive features of hydrogel materials and nanoparticles, such as good biocompatibility, tailorable biodegradability, easy chemical modification, high responsiveness, high colloidal stability, and the possibility of targeted delivery of loaded therapeutics after intravenous administration.[22] Therefore nanogels have distinct advantages over other types of nanomaterials for biomedical applications.[23] Moreover, by varying the chemical composition of nanogels, their characteristics such as size, charge, porosity, amphiphilicity, softness, and degradability can be fine-tuned and tailored. Our previous study has shown that pHEMAm-Gly-HEMAm nanogels are cytocompatible and their degradation can be tailored depending on the crosslink density of nanogels.[19] Therefore, PEGylated biodegradable p(HEMAm-co-AzEMAm)-Gly-HEMAm-based nanogels that require in vitro optimization of their degree of PEGylation and crosslink density (**Figures 1** and **2**) were used as an example. To study the effect of PEG density on particle size, dynamic light scattering (DLS) was used (**Figure 3**A). The stability/aggregation of nanogels upon incubation in human plasma was further studied by fluorescence single particle tracking (fSPT) (Figure 3B). Tangential flow filtration (TFF) was used as an artificial circulating system to mimic the degradation of PEGylated nanogels with different crosslink densities and filtration of the soluble degradation products from the system in vitro (Figure 3C). The degradation behavior of PEGylated nanogels with optimized PEG and crosslink densities in phosphate buffered saline (PBS) and undiluted human plasma were compared using fluorescence fluctuation spectroscopy (FFS) (Figure 3D).

2. Experimental Section

2.1. Materials

N-(2-hydroxyethyl)methacrylamide (HEMAm), HEMAm-oligoglycolates (HEMAm-Gly, degree of polymerization 1.83), and *N*-(2-azidoethyl)methacrylamide (AzEMAm) were synthesized as previously described.[19,24–26] BCN-PEG$_{5000}$-OMe was purchased from SynAffix BV (Oss, the Netherlands). Irgacure 2959 was obtained from Ciba Specialty Chemicals Inc. (Hercules, USA). ABIL EM 90 was provided from Evonik Industries AG (Essen, Germany). Alexa Fluor 488 DIBO alkyne was purchased from Thermo Fisher (Bleiswijk, the Netherlands). Acetonitrile, dichloromethane, dimethylformamide, ethyl acetate, methanol, hexane, and dimethyl sulfoxide (DMSO) were obtained from Biosolve (Valkenswaard, the Netherlands). Poly(ethylene oxide) standard (M_n: 19 kDa, PDI: 1.04) for Viscotek calibration was from Malvern Instruments Ltd (Worcestershire, UK). All other chemicals and reagents were obtained from Sigma-Aldrich (Zwijndrecht, the Netherlands).

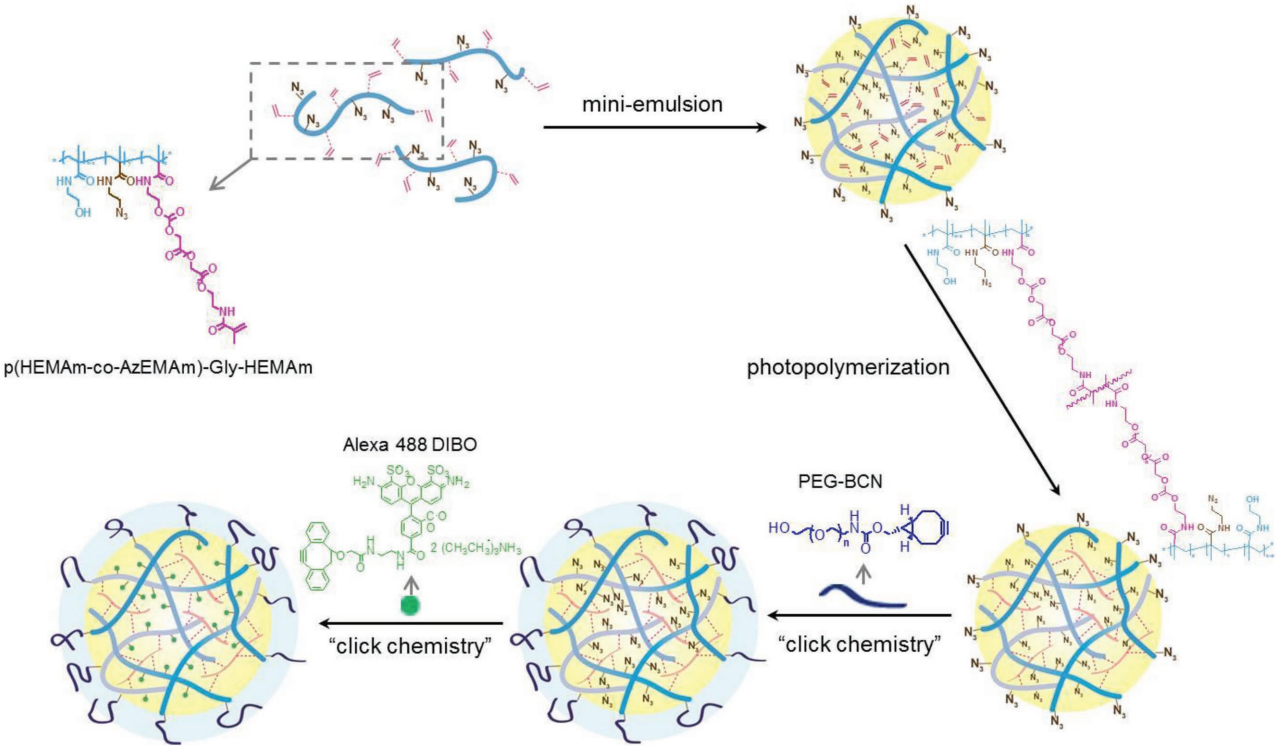

Figure 2. Preparation of PEGylated Alexa 488 labeled nanogels.

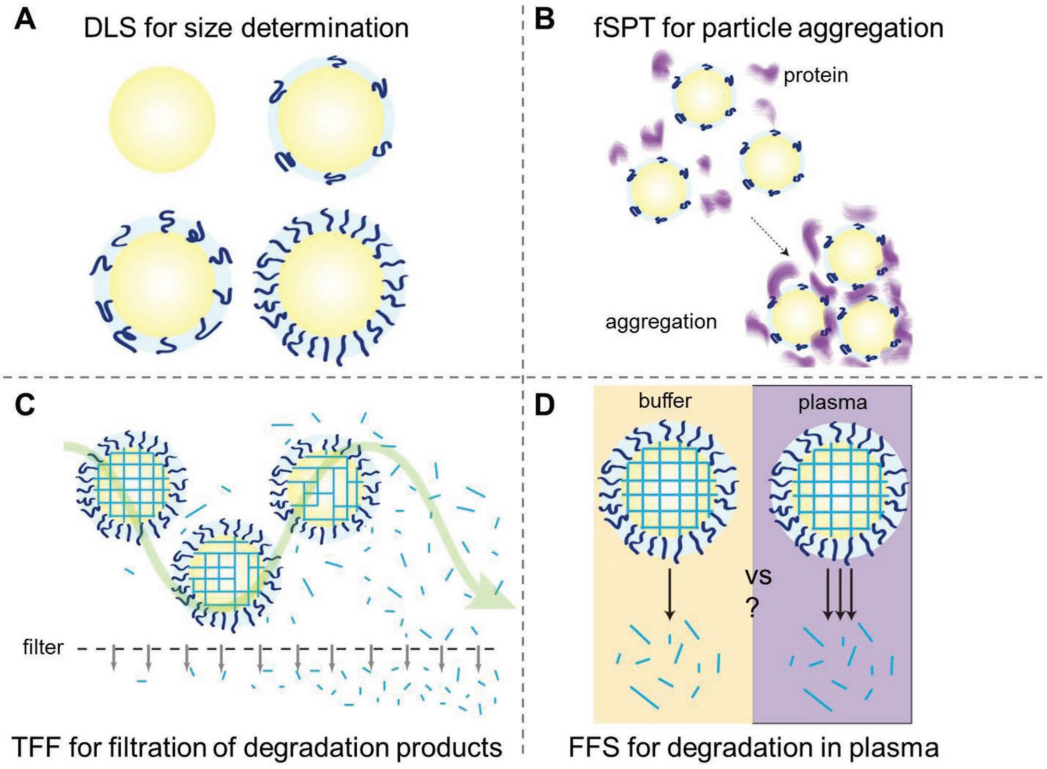

Figure 3. Characterizations of A) unlabeled nanogels (DS 5–10, 5–20% AzEMAm%) before and after PEGylation by DLS, B) Alexa 488 labeled nanogels (DS 20, 5–20% AzEMAm%) before and after PEGylation by fSPT, C) Alexa 488 labeled PEGylated nanogels (DS 5–20, 20% AzEMAm%) by TFF, and D) Alexa 488 labeled PEGylated nanogels (DS 10, 20% AzEMAm%) by FFS.

2.2. Synthesis of Copolymer p(HEMAm-co-AzEMAm)

The synthesis of azide functionalized copolymers, p(HEMAm-co-AzEMAm) (5–20 mol% of AzEMAm), was performed by free radical polymerization using HEMAm and AzEMAm as monomers and 4,4-azobis(4-cyanopentanoic acid) (ABCPA) as the initiator (molar ratio of monomer/initiator was 15:1) according to a previously published procedure. Briefly, the monomers and initiator were dissolved in deionized water at a total concentration of 25 mg mL^{-1}. After flushing with N_2 for 30 min at room temperature, the solution was heated to 70 °C and stirred for 24 h. The products were purified by dialysis (membrane cutoff 3500 Da) against deionized water and recovered after freeze drying.

2.3. Characterization of Copolymers

After polymerization, a sample of the reaction solution (5 µL) was injected into a Waters ACQUITY UPLC system (Waters Associates Inc. Milford, MA) to determine the concentrations unreacted HEMAm and AzEAMm, using an Acquity BEH C18 column 1.7 µm (2.1 × 50 mm). The measurement was performed using 10×10^{-3} M $HClO_4$/acetonitrile (95/5, v/v) eluent A and 10×10^{-3} M $HClO_4$/acetonitrile (5/95, v/v) as eluent B. After an isocratic flow of eluent A for 1 min, a gradient was run from 100% to 50% eluent A in 2 min with a flow rate of 0.5 mL min^{-1}. The detection wavelength was 210 nm. The retention times of HEMAm and AzEMAm were 0.78 and 2.11 min, respectively. Calibration curves were linear between 0.01 and 10 µg mL^{-1} for both HEMAm and AzEMAm. The areas of HEMAm and AzEMAm under the curve were recorded and the conversions of monomers were calculated according to Equation (1)

$$\text{Conversion}\,(\%) = \left(1 - \frac{\text{amount of unreacted monomer}}{\text{total amount of added monomer}}\right) \times 100\% \quad (1)$$

The obtained copolymers were characterized by Fourier-transform infrared spectroscopy (FT-IR) analysis using KBr pellets with a BIO-RAD FTS6000 FT-IR (BIO-RAD, Cambridge, MA, USA) instrument. Solid state spectra of the polymer were acquired by accumulating 32 scans per spectrum at a data point resolution of 2 cm^{-1}.

The copolymer composition of the synthesized polymers was quantified by dissolving samples in deuterium oxide and analyzed by ^{1}H-NMR. The spectra were recorded with an Agilent 400-NMR spectrometer (Santa Clara, CA, USA). The central line of deuterium oxide at 4.75 ppm was used as reference line. The integral intensities $I_{3.46}$ and $I_{3.65}$ of protons at 3.46 ppm (AzEMAm) and 3.65 ppm (HEMAm) were recorded and the mol% of AzEMAm in polymers was calculated according to Equation (2)

$$\text{Mol\%}_{\text{AzEMAm}} = \frac{I_{3.46}}{I_{3.46} + I_{3.65}} \times 100\% \quad (2)$$

Molecular weight and molecular weight distribution of the synthesized polymers were determined by Viscotek TDAmax (equipped with RI, light scattering, and viscosity detectors, Malvern Instruments Ltd., UK) with two PL aquagel-OH 30 columns (Agilent, USA). A 0.3 M sodium acetate buffer (pH 6.5) was used as the eluent with a flow rate of 0.7 mL min^{-1}. Samples were dissolved in the mobile phase at the concentration of 2 mg mL^{-1} and injected onto the column (injection volume 100 µL). Results were analyzed by OmniSEC software (Malvern Instruments Ltd., UK) with poly(ethylene oxide) (M_n: 19 kDa, PDI: 1.04, Malvern Instruments Ltd., UK) as the calibration standard.

2.4. Labeling of Copolymer

A labeled copolymer was obtained by copper-free click chemistry reaction between the azide groups of copolymer and DIBO groups of Alexa 488 DIBO. Briefly, 10 mg copolymer (containing 20 mol% AzEMAm) was dissolved in 1 mL of ammonium acetate buffer (100×10^{-3} M, pH 5) and 10 µL of Alexa 488 DIBO (1 mg mL^{-1} in DMSO) was added. The mixture was stirred at room temperature for 1 h. The labeled copolymer was purified by PD 10 chromatography and recovered after freeze drying.

2.5. Synthesis of p(HEMAm-co-AzEMAm)-Gly-HEMAm

P(HEMAm-co-AzEMAm)-Gly-HEMAm with degrees of substitution (DS, the number of methacryloyl groups per 100 HEMAm units) of ≈5, 10, and 20 were prepared as previously described.[19,24] Briefly, 1,1′-carbonyldiimidazole (CDI)-activated HEMAm-Gly (HEMAm-Gly-CI) was obtained by reaction of the hydroxyl group of HEMAm-Gly (degree of polymerization 1.83) with CDI. Subsequently, HEMAm-Gly-CI was coupled to p(HEMAm-co-AzEMAm) in the presence of DMAP.

2.6. Preparation, PEGylation, and Labeling of Empty Nanogels

The preparation of empty nanogels was carried out according to previous studies.[19,27] In brief, p(HEMAm-co-AzEMAm)-Gly-HEMAm (37.5 mg) dissolved in DMSO (212.5 µL) was mixed with Irgacure 2959 (150 µL, 10 mg mL^{-1} in distilled water). The mixture was added to 5 mL of mineral oil (containing 10%, v/v ABIL EM 90) and subsequently vortexed. The formed emulsion was further sonicated by a tip sonicator (Bandelin Sonopuls, pulse on/off 0.5 s, and amplitude 10%) for 15 min and irradiated under UV (940 mW cm^{-2}, 300–650 nm, Bluepoint UVC source, Honle UV technology, German) for 15 min. Next, the emulsion was mixed with 40 mL acetone and centrifuged. The pellet was further washed with 40 mL acetone/hexane (1:1, v/v) for four times. After the organic solvent was removed under vacuum, the pellet was redispersed in water and lyophilized.

To modify nanogels with PEG, 10 mg of freeze dried nanogels was dispersed in 1 mL of ammonium acetate buffer (100×10^{-3} M, pH 5) and PEG_{5000}-BCN solution (10 mg mL^{-1} in pH 5 ammonium acetate buffer) was added. The volume of PEG_{5000}-BCN solution was 0.25, 0.5, and 1 mL for nanogels prepared from copolymers with 5, 10, or 20 mol% of AzEMAm, respectively, to make sure the molar ratio of PEG to azide groups (1:10) was the same for the different copolymers. The mixture was stirred at room temperature for 4 h, followed by ultracentrifugation (250 000 × g for 1 h) to remove unreacted PEG-BCN.

The PEGylation efficiency was determined by measuring the amount of unreacted PEG_{5000}-BCN in the supernatant after ultracentrifugation. The determination was performed by Viscotek TDAmax with a PL aquagel-OH 30 column, using ammonium acetate buffer (100×10^{-3} M, pH 5) as the eluent. The flow rate was 0.7 mL min^{-1} and the injection volume was 100 µL and the light scattering signal was recorded. The calibration curve of PEG_{5000}-BCN was linear between 1 and 10 mg mL^{-1}. The PEGylation efficiency was calculated according to Equation (3)

$$\text{PEGylation efficiency (\%)} = \left(1 - \frac{\text{amount of unreacted } PEG_{5000}\text{-BCN}}{\text{amount of added } PEG_{5000}\text{-BCN}}\right) \times 100\% \quad (3)$$

Labeling of PEGylated and non-PEGylated nanogels with Alexa 488 was performed according to a previously reported procedure.[26] Freeze dried nanogels (10 mg) were dispersed in 1 mL of ammonium buffer (100×10^{-3} M, pH 5) and 10 µL of Alexa 488 DIBO (1 mg mL^{-1} in DMSO) was added. The mixture was stirred at room temperature for 1 h. The labeled nanogels were purified by PD 10 chromatography and recovered after freeze drying.

The size and size distribution of re-suspended nanogels (0.5 mg mL^{-1} in 20×10^{-3} M HEPES pH 7.4) were measured by DLS (Malvern ALV/CGS-3 Goniometer, Malvern, UK) at 25 °C. The zeta potential of nanogels in 20×10^{-3} M HEPES (pH 7.4) was measured using a Malvern Zetasizer Nano-Z (Malvern, UK) at 25 °C.

2.7. Stability of Nanogels Using fSPT

fSPT assay was carried out to study the stability/aggregation of DS 20 nanogels with different PEGylation degrees in full human plasma. A custom-built laser widefield epifluorescence microscope was set up as described by Braeckmans et al.[28] Labeled nanogels (concentration of 10^9 to 10^{12} particles per mL) were incubated in human plasma for 1, 2, 3, and 4 h at 37 °C. At each time point, 5 µL of sample was taken and introduced in a microscope slide and cover glass with double-sided adhesive tape. The samples were excited using widefield laser illumination. Movies of individual nanogels diffusing in the medium (10–20 movies of 8 s per sample) were recorded and analyzed using custom-developed software. By calculating the diffusion coefficient for each trajectory, the size distribution of nanogels in the medium was obtained after transformation of obtained distribution of empirical diffusion coefficients using the Stokes–Einstein equation.[28] The viscosity of human plasma was set to 1.35 cP at 37 °C for the calculations. The size distribution of nanogels in PBS (pH 7.4, containing 0.049 M NaH_2PO_4, 0.099 M Na_2HPO_4, and 0.006 M NaCl) was measured as a control.

2.8. Degradation and Filtration of Nanogels by TFF

The KR2*i* TFF system (Spectrum Laboratories Inc., Breda, the Netherlands) was set up with a pump, a sample reservoir, a buffer reservoir, and a hollow fiber filter module (mPES, molecular weight cutoff (MWCO) 50 kDa, surface area 20 cm^2) as shown in **Figure 4**A. The experiment was performed in PBS (pH 7.4, containing 0.049 M NaH_2PO_4, 0.099 M Na_2HPO_4, 0.006 M NaCl) containing 0.5 wt% Tween 20 and the processing volume was 15 mL. The retentate was directed back to the sample reservoir and fresh eluent was fed into the sample reservoir from the buffer reservoir at the same rate as filtrate was being generated to maintain the constant volume in the system. The experiment was done at 37 °C with flow rate 15 mL min^{-1} and operating pressure 10–20 psi. Before the experiment, the whole system was washed with 0.05 M NaOH and rinsed with deionized water thoroughly. Afterward, the system was flushed with PEGylated nanogel suspension (20%, DS 20, 0.2 mg mL^{-1} in the eluent) overnight to avoid unspecific binding of the labeled nanogels to the system. Then, the eluent was refreshed and Alexa 488 labeled polymer or Alexa 488 labeled PEGylated nanogel suspension (20%, DS 5, 10, and 20) was added to the final volume 15 mL and concentration 0.2 mg mL^{-1}. The filtration was performed for 3 d. At designated time points, the volume of retentate was recorded and 0.5 mL retentate samples were taken. The samples were further incubated in an oven at 37 °C with a total of 144 h incubation time (during TFF and in the oven) to degrade the remaining particles[19] and analyzed using JASCO FP8300 spectrofluorometer (JASCO Benelux B.V., IJsselstein, the Netherlands). The fluorescence intensity ($\lambda_{ex.}$ = 495 nm, $\lambda_{em.}$ = 519 nm) was recorded and the concentration was calculated according to the calibration curve of Alexa 488 DIBO (linear at a concentration ranging from 0.01 to 1 µg mL^{-1}). The normalized amount of materials in the retentate was calculated using Equation (4)

$$\text{Normalized amount of materials in the retentate (\%)} = \frac{C_{tr} \times V_{tr}}{C_{0r} \times V_{0r}} \times 100\% \quad (4)$$

Where C_{tr} and V_{tr} are the concentrations of materials in the retentate and the volume of retentate at sampling time, respectively; C_{0r} and V_{0r} are the concentration of materials in the retentate and the volume of retentate at time 0, respectively.

As a control, Alexa 488 labeled p(HEMAm-co-HEMAm) was added to the DS 20 nanogels treated system and TFF experiment was performed for 4 h under the same conditions as nanogels. At different time points, the volumes of filtrate and retentate were recorded. Then, the filtrate and 0.5 mL of the retentate were collected and measured by JASCO FP8300 spectrofluorometer ($\lambda_{ex.}$ = 495 nm, $\lambda_{em.}$ = 519 nm) using the calibration curve of Alexa 488. The normalized amount of polymer in the retentate was calculated based on Equation (4) and the normalized amount of polymer in the filtrate was calculated using Equation (5)

$$\text{Normalized amount of materials in the filtrate (\%)} = \frac{C_{tf} \times V_{tf}}{C_{0r} \times V_{0r}} \times 100\% \quad (5)$$

where C_{tf} and V_{tf} are the concentration of the polymer in the filtrate and the volume of filtrate at sampling time, respectively; C_{0r} and V_{0r} are the concentration of the polymer in the retentate and the volume of retentate at time 0, respectively.

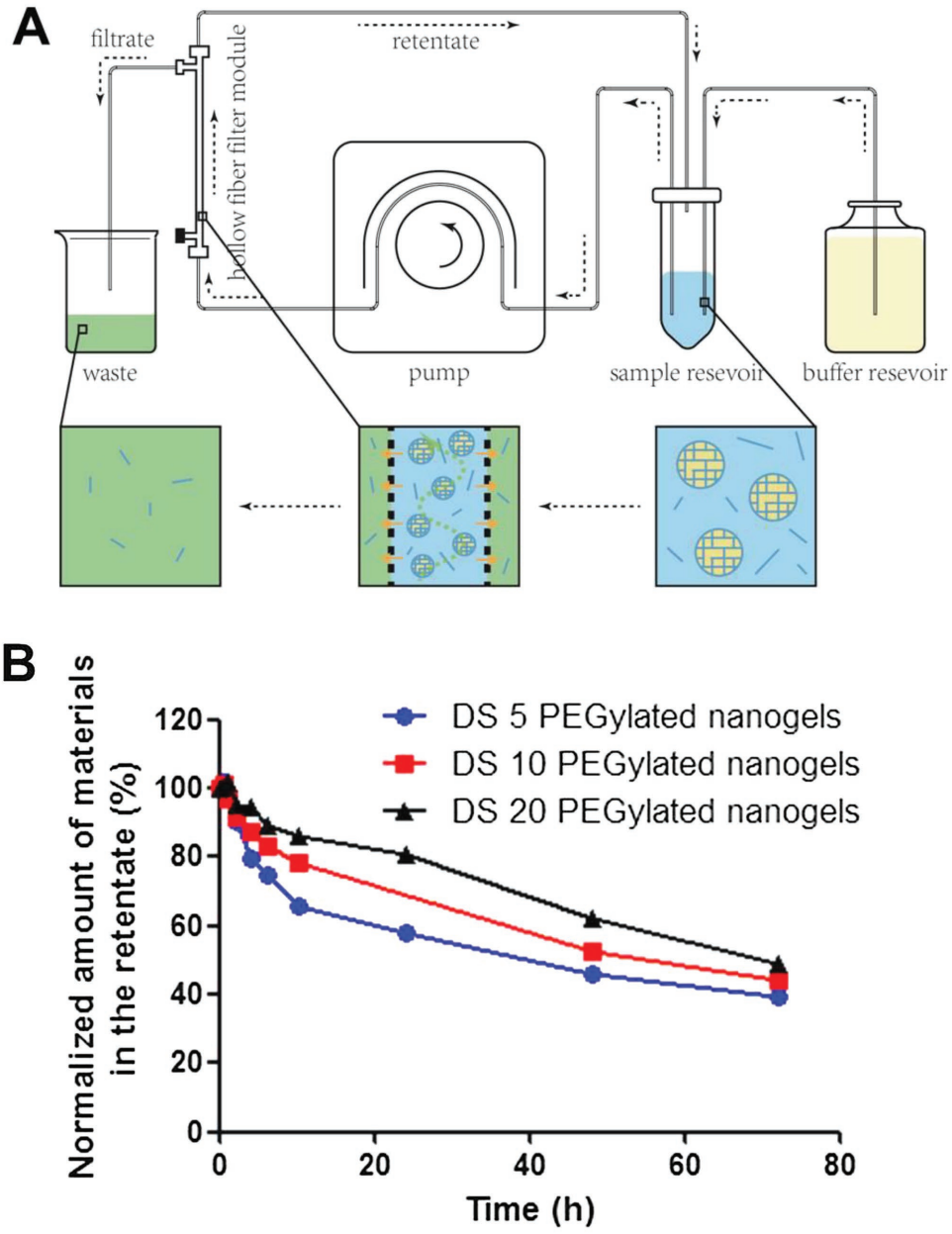

Figure 4. A) Experimental setup used for TFF. B) Normalized amount of materials in the retentate after Alexa 488 labeled p(HEMAm-co-AzEMAm) nanogels prepared from different DS polymers circulated in TFF system (pretreated by DS 20 PEGylated nanogels) at 37 °C over time.

The molecular weight and molecular weight distribution of polymer in the retentate after different filtration times were determined by Viscotek TDAmax with two PL aquagel-OH 30 columns, using PBS as the eluent (see Section 2.4).

2.9. Degradation of Nanogels Using Fluorescence Fluctuation Spectroscopy

The degradation of nanogels during 24 h incubation in PBS (pH 7.4) or in human plasma at 37 °C was determined by fluorescence fluctuation spectroscopy (FFS). FFS is able to monitor the fluorescence intensity fluctuations of molecules diffusing in and out of the focal volume of a confocal microscope. When free labeled polymers during nanogel degradation are dissolved in the confocal volume, a fluorescence signal (baseline) proportional to the concentration of polymers can be obtained. As the complete degradation control, nanogel suspension was incubated in sodium borate buffer (100×10^{-3} M, pH 9) at the same concentration in PBS or plasma at 37 °C for 6 h. The procedure was similar as previously described by Buyens et al.[29] and Novo et al.,[30] with some modifications. Briefly, FFS measurements were performed on Alexa 488 labeled PEGylated nanogels (20%, DS 10) ($\lambda_{ex.} = 495$ nm, $\lambda_{em.} = 519$ nm) on a C1si laser scanning confocal microscope (Nikon, Japan), equipped with a time-correlated single photon counting

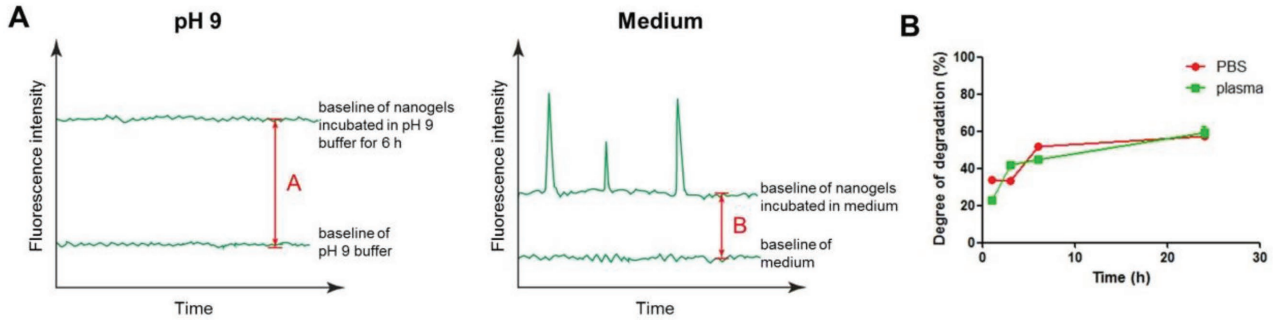

Figure 5. A) Schematic representation of the fluorescence fluctuation profiles recorded for pH 9 buffer and nanogels incubated in pH 9 buffer for 6 h, and for the medium (PBS or human plasma) and nanogels incubated in medium. B) Degree of degradation of PEGylated DS 10 nanogels incubated in PBS (pH 7.4) or human plasma for 24 h, as measured by FFS.

Data Acquisition module (PicoQuant, Berlin, Germany), and water immersion objective lens (Plan Apo 60 ×, NA 1.2, collar rim correction, Nikon, Japan). During the measurements, the glass bottom 96-well plate (Grainer Bio-one, Frickenhausen, Germany) was covered with Adhesive Plates Seals (Thermo-Scientific, UK) to avoid evaporation of water. For each sample, fluorescence intensity fluctuations (**Figure 5**A) were recorded using Symphotime (PicoQuant, Berlin, Germany), during 1 min in triplicates. As the baseline fluorescence intensity of the fluorescence fluctuation profiles recorded by FFS is proportional to the concentration of formed free polymer during nanogel degradation, the degree of degradation can be calculated using Equation (6)

$$\text{Degree of degradation} = \frac{B}{A} \times 100\% \quad (6)$$

where A is the difference in fluorescence intensity between baseline of pH 9 buffer and nanogels incubated in pH 9 buffer for 6 h, and B is the difference in fluorescence intensity between baseline of medium (PBS or human plasma) and nanogels incubated in medium for different time.

3. Results and Discussion

3.1. Synthesis and Characterization of p(HEMAm-co-AzEMAm)-Gly-HEMAm

P(HEMAm-co-AzEMAm)-Gly-HEMAm with various contents of AzEMAm and different DS of Gly-HEMAm side units (Figure 1) were synthesized to investigate the stability and degradation of nanogels based on these polymers with different degrees of PEGylation and crosslink densities.

The polymers were synthesized in two steps. First, p(HEMAm-co-AzEMAm) with different AzEMAm (5–20 mol%) was synthesized by free radical polymerization using HEMAm and AzEMAm as monomers and ABCPA as initiator (Figure S1A, Supporting Information).[26] The ^{1}H-NMR spectra of p(HEMAm-co-AzEMAm) displayed a resonance peak of AzEMAm group at 3.46 ppm (Figure S1B, Supporting Information). The characteristics of the obtained copolymers are summarized in **Table 1**. All copolymers were obtained with good yields (>80%) as reported previously.[26] The number average molecular weight ranged from 10 to 15 kDa, which is smaller than kidney elimination threshold (45 kDa),[31] with a PDI around 3. Complete conversions of HEMAm (98%) and AzEMAm (99%) were obtained after polymerization and the ratio of HEMAm to AzEMAm in the copolymer was the same as the feed ratio for all copolymers. IR analysis further showed a characteristic peak at 2100 cm^{-1} of the azide vibration, the intensity of which increased with increasing AzEMAm content (Figure S1C, Supporting Information).

The copolymers were further modified with crosslinkable methacrylamide side unit, which contains hydrolytically biodegradable ester bonds (Figure S1A, Supporting Information).[32] Copolymers with three different DSs (5, 10, and 20) were synthesized for each p(HEMAm-co-AzEMAm) and thus nine different p(HEMAm-co-AzEMAm)-Gly-HEMAm were obtained.

3.2. Preparation, PEGylation, and Labeling of Nanogels

Nanogels with different crosslink densities and contents of AzMEAm were obtained with a yield around 80%. Afterward, PEG_{5000}-BCN was conjugated to the surface of nanogels by copper-free click chemistry reaction (i.e., strain-promoted azide-alkyne cycloaddition) of azide and BCN groups under mild reaction conditions.[33] This reaction not only has the benefits of normal click chemistry such as high reactivity and selectivity,[34] but also avoids the use toxic metal catalyst.[35] The properties of nanogels are summarized in **Table 2**. Before

Table 1. Characteristics of p(HEMAm-AzEMAm) as determined by ^{1}H-NMR, UPLC, and GPC.

HEMAm/AzEMAm [mol/mol in the feed]	Yield [%]	Conversion [%][a)]		Copolymer composition[b)]	M_n[c)] [kDa]	PDI
		HEMAm	AzEMAm			
95/5	85.6	98.4	99.6	94/6	10.2	3.5
90/10	84.0	98.5	99.2	89/11	11.2	3.6
80/20	93.2	98.8	99.1	79/21	14.6	3.0

[a)]Determined by ^{1}H-NMR; [b)]Determined by UPLC; [c)]Determined by GPC.

Table 2. Properties of nanogels before and after PEGylation ($n = 3$).

DS	AzEMAm%	Yield [%]	PEGylation	Size [nm]	PDI	Zeta potential [mV]	PEGylation efficiency [%]	PEG content [mg/mg nanogels]
5	5	93.1 ± 5.4	Before	203 ± 5	0.27 ± 0.02	−2.7 ± 0.3	–	–
			After	208 ± 3	0.21 ± 0.01	−2.4 ± 0.4	38.2 ± 5.4	0.10 ± 0.01
	10	79.7 ± 3.5	Before	198 ± 4	0.17 ± 0.00	−2.6 ± 0.1	–	–
			After	209 ± 6	0.19 ± 0.02	−2.4 ± 0.3	51.9 ± 4.8	0.26 ± 0.02
	20	86.1 ± 3.1	Before	170 ± 4	0.16 ± 0.02	−2.7 ± 0.2	–	–
			After	193 ± 4	0.18 ± 0.02	−2.6 ± 0.2	67.3 ± 7.9	0.67 ± 0.08
10	5	83.7 ± 4.3	Before	170 ± 5	0.21 ± 0.03	−2.7 ± 0.1	–	–
			After	174 ± 4	0.25 ± 0.01	−2.6 ± 0.4	35.7 ± 3.5	0.09 ± 0.01
	10	88.8 ± 5.1	Before	199 ± 5	0.18 ± 0.03	−2.9 ± 0.3	–	–
			After	209 ± 5	0.22 ± 0.02	−2.5 ± 0.1	48.5 ± 4.0	0.24 ± 0.02
	20	88.8 ± 4.1	Before	238 ± 4	0.13 ± 0.01	−2.5 ± 0.3	–	–
			After	257 ± 6	0.17 ± 0.01	−2.3 ± 0.2	61.7 ± 2.1	0.62 ± 0.02
20	5	96.2 ± 4.9	Before	254 ± 6	0.13 ± 0.00	−2.7 ± 0.3	–	–
			After	259 ± 7	0.16 ± 0.01	−2.6 ± 0.3	38.5 ± 1.7	0.10 ± 0.00
	10	86.7 ± 6.0	Before	234 ± 5	0.19 ± 0.01	−2.8 ± 0.2	–	–
			After	246 ± 4	0.21 ± 0.02	−2.7 ± 0.2	55.8 ± 2.9	0.28 ± 0.01
	20	95.2 ± 2.4	Before	233 ± 5	0.18 ± 0.02	−2.8 ± 0.1	–	–
			After	254 ± 5	0.18 ± 0.00	−2.6 ± 0.3	67.7 ± 6.7	0.68 ± 0.07

PEGylation, the size of nanogels ranged from 160 to 230 nm with PDI of about 0.2 and the particles were neutral at pH 7.4. After PEGylation, the zeta potential did not change whereas the size of the nanogels slightly increased (e.g., from about 203 to 208 nm for DS 5 and 5% nanogels) after PEGylation due to the thickness of the PEG layer. Besides, the difference in size before and after PEGylation increased with an increasing PEG content; e.g., looking at the DS 5 nanogels (Table 2) one can find that PEGylation increases the particle size by 5, 10, and 20 nm for nanogels containing 5%, 10% and 20% AzEMAm%, respectively. Many studies have shown that PEG chains have a "mushroom" conformation when the surface density is low, while the chains are forced in a "brush" conformation at high surface densities leading to an increase of layer thickness from 10 to 20 nm (5 kDa PEG).[10,13,36]

PEGylated and non-PEGylated nanogels were further labeled with Alexa 488 using copper-free click chemistry reaction between the DIBO group of the dye and the remaining azide groups of nanogels, and the labeling efficiency was over 80% (Figure S2, Supporting Information). These labeled nanogels were used for further studies.

3.3. Stability of Nanogels Using fSPT

fSPT has shown its superiority over DLS to study possible aggregation of nanoparticles in biological fluids by excluding the effect of scattering from proteins in biofluids.[37] This technique records the movement of individual fluorescently labeled nanoparticles, calculates the diffusion coefficient based on the their trajectories, and converts this to the size distribution of dispersed nanoparticles.[28] Therefore, fSPT was used to evaluate the influence of PEGylation on the colloidal stability of the nanogels in undiluted human plasma. Alexa 488 labeled nanogels (DS 20) with different degrees of PEGylation were incubated at 37 °C in human plasma. Nanogels with the highest crosslink density (DS 20) and thus highest stability[19,27] were chosen in this study to minimize the effect of nanogel degradation on particle aggregation during the stability study. The size distribution of nanogels in plasma was determined by fSPT after different incubation times and compared with that of nanogels dispersed PBS buffer (pH 7.4) (**Figure 6**). The size distributions of DS20 nanogels in PBS measured by fSPT were comparable to that obtained from DLS data (average size ranged from 250 to 300 nm). fSPT analysis showed a change in particle size distribution upon incubation in human plasma at 37 °C over time. Increased colloidal stability was observed with an increasing degree of PEGylation of the nanogels. For non-PEGylated 5% nanogels (Figure 6A), the average size increased from 250 to over 1000 nm after 1 h incubation in plasma. After 2 h incubation, complete aggregation was observed and the sample was not suitable for further quantitative measurements. For nanogels with 5% PEGylation, which is the lowest PEGylation degree, the average size of particles increased from 250 to 700 nm after 4 h incubation in plasma at 37 °C (Figure 6B). The size distribution was much broader than at the start of the experiment. It has been shown that protein adsorption contributes to aggregation of nanocarriers.[38,39] This result demonstrates that this degree of PEGylation (5%) cannot fully prevent protein absorption. For nanogels with 10% PEG_{5000}, a clear change of size distribution can already be seen after 1 h incubation in plasma (Figure 6C) and an increased average size (460 nm) and large aggregations (>500 nm) were observed after 2 and 3 h of incubation, respectively. Nanogels with the highest

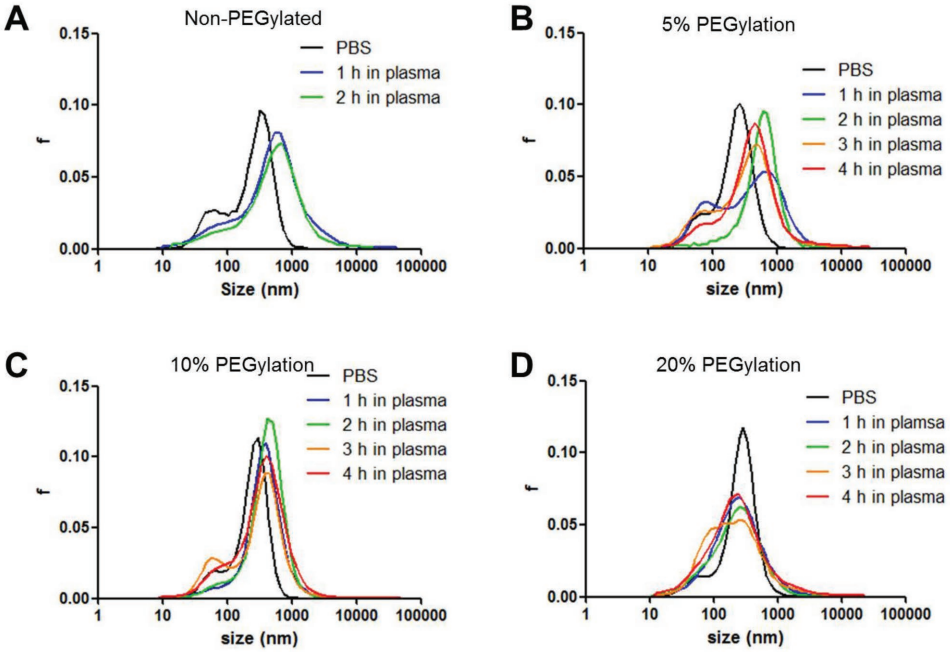

Figure 6. Size distribution of A) non-PEGylated 5% nanogels, B) PEGylated 5% nanogels, C) PEGylated 10% nanogels, and D) PEGylated 20% nanogels as determined by fSPT after incubation in full human plasma at 37 °C. Size distribution was also determined in PBS (pH 7.4).

degree of PEGylation (PEGylated 20% nanogels) showed only a slight change of the size distribution after 1 h incubation (Figure 6D). Furthermore, no significant change of size distribution was found during further incubation until 4 h and no particle aggregates were detected. This result also confirms the hypothesis from DLS data that PEGylated 20% nanogels had the highest colloidal stability and the best anti-aggregation ability. Interactions between particles with high degree of PEGyation and proteins are decreased due to the shielding properties of the PEG layer, which results in the successful stabilization of colloidal particles in biofluids. The nanogels with 20% PEGylation are expected to show less plasma protein binding and therefore a reduced recognition by the mononuclear phagocyte system and longer circulation time.[8,10,40] Therefore, nanogels with 20% PEG and with different crosslink densities were further studied.

3.4. Degradation and Filtration of Nanogels by TFF

Nanogels prepared from building blocks of different degrees of substitution (Figure 1) have different crosslink densities, which in turn lead to different degradation kinetics.[19,41] When they are i.v. injected, they slowly degrade, finally yielding p(HEMAm-co-AzEMAm) of which the average molecular is 10 kDa, which is lower than the renal elimination threshold (around 45 kDa) and thus can be potentially excreted by the kidneys.[31,42] As one of the main membrane filtration techniques, TFF (or cross flow filtration) has been used for decades to purify and concentrate biotherapeutics in the pharmaceutical industry.[43] Equipped with filters with different MWCO, TFF also enables purification,[44,45] size selection,[46] and concentration[47] of nanoparticles.

Since membrane separation is the principle of renal filtration for nanocarrier clearance,[48] TFF was used as an artificial circulation and filtration system to predict the circulation times of nanogels with different crosslink densities in vitro (Figure 4A). The MWCO of the filter was chosen as 50 kDa, which is close to the threshold for renal filtration.[31] The surface area of the filter (20 cm^2), process volume (15 mL), and flow rate (15 mL min^{-1}) was close to total glomerular capillary surface area, blood volume, and flow rate in a healthy rat.[49–52] During the experiment, the nanogel suspension continuously circulated in the system. Upon incubation, the degradation fragments with molecular weight smaller than MWCO of the filter were filtered out from the system by transmembrane pressure (pressure difference between feed and permeate pressure).

When a DS 20 nanogel suspension was added to an untreated TFF system, a dramatic decrease of fluorescence intensity of retentate was observed (fluorescence intensity decreased by about 40% in the first 2 h). Given that DS 20 nanogels have slow degradation,[19] the decrease of fluorescence intensity is probably due to unspecific adsorption of nanogels onto tubes and filter membrane. Therefore, the system was first saturated with DS 20 nanogels overnight to block unspecific binding. Alexa 488 labeled p(HEMAm-co-AzEMAm) (20% AzMEAm%, M_n: 10.2 kDa, PDI: 3.5) was used to confirm that after blocking process the filter was still able to filter the degradants (i.e., soluble polymers) based on molecular weight. Figure S3 (Supporting Information) shows that in time, the amount of polymer in the filtrate increased and its amount in the retentate decreased accordingly. The recovery of fluorescence was over 90% during the experiment, indicating that a specific binding of the polymer was minimized. After 4 h filtration, almost 80% of the fed polymer was permeated from the circulation and filtered out. Table S1 (Supporting Information)

shows that the molecular weights of the soluble polymers in the filtrate increased slowly and the number average molecular weights were smaller than 50 kDa. The result is in line with the observation of other in vivo studies that around 50% of poly(*N*-(2-hydroxypropyl) methacrylamide) (pHPMA) (M_n 21.8 kDa, PDI 1.7) was excreted from the kidneys after 3 h intravenous administration.[31,53] After 4 h filtration, more than 20% the polymers retained in the retentate and the number average molecular weight was around 80 kDa with narrow PDI (<1.2) (Table S1, Supporting Information). These results demonstrate that the filter is able to separate polymers based on the differences of molecular weight: small polymers can pass through the membrane and chains with molecular weights higher than MWCO can be intercepted in the retentate.

After evaluation of the selectivity of filter membrane, the degradation of nanogels and anticipated clearance of degradants from the pretreated TFF system was studied (Figure 4B). Since nanogels prepared from polymers with 20% AzEMAm% showed the highest colloidal stability in human plasma after PEGylation by fSPT, nanogels with highest degree of PEGylation (20% AzEMAm%) and various crosslink densities (DS 5, 10, 20) were used in this study. The decrease of amount of the retentate was found for all nanogels, indicating that during incubation and circulation, the degradation products could be filtered and removed from the system. Fast filtration was found at the beginning of the experiment (<10 h incubation).Thereafter, the normalized amounts of materials in the retentate were 60% for DS5, 80% for DS 10, and 85% for DS 20 nanogels, respectively. Additionally, a more rapid decrease of the amount of materials was found for nanogels prepared from a lower DS polymer. For example, the normalized amounts of materials in the retentate were about 45% for DS 5, 50% for 10 nanogels, and more than 60% for DS 20 nanogels after 72 h of incubation. This demonstrates that nanogels with lower crosslink density have faster degradation and were consequently more rapidly removed by filtration. Compared to the degradation behavior of nanogels with the same crosslink density, which was measured by DLS in the previous study,[19] the decrease of filtration rate obtained by TFF was slower: After 48 h incubation, normalized light scattering intensity of nanogel suspension dropped to 20% for DS 5 and 10 nanogels, and 40% for DS 20 nanogels as measured by DLS.[19] A possible explanation is that the dissolved fragments from nanogel degradation (which have much weaker light scattering) need to be further hydrolyzed into small fragments and only polymer chains with molecular weight smaller than MWCO can be filtered.[54] Therefore, TFF is able to clearly characterize the degradation behavior of nanogels in terms of crosslink density and can be used as an in vitro tool to predict the in vivo degradation behavior of nanogels.

3.5. Fluorescence Fluctuation Spectroscopy

FFS was chosen to study the degradation behavior of the nanogels in human plasma and PBS. FFS has been previously exploited to study the stability/dissociation of siRNA-polymer complexes in biofluids.[29,30] In these studies it was shown that the baseline fluorescence intensity of the fluctuation profile is proportional to the free fluorophore-labeled siRNA concentration released from complexes. In the present study this principle was applied to in vitro characterize and predict the in vivo degradation behavior of nanogels. The triazole linkages between the dye and polymer formed by click reaction between azides and alkynes are known to be stable under physiological conditions.[55,56] Therefore, the detected fluorescence is due to the polymer bound dye and not to the free dye. As shown in fSPT study, nanogels with the highest degree of PEGylation revealed the highest colloidal stability in human plasma. Furthermore, nanogels with medium crosslink density (prepared from DS 10 polymers) showed optimal degradation behavior in vitro by TFF. Therefore, Alexa 488 labeled, PEGylated nanogels prepared from the DS 10 and 20% AzEMAm% polymer were chosen to study the effect of their degradation behavior both in plasma and buffer. At time 0, the low baseline suggests that very little labeled free polymer was present (Figure S4A, Supporting Information). The more intense fluorescence peaks are due to the diffusion of Alexa 488 labeled nanogels in and out of the excitation volume. During the incubation, the nanogels slowly degrade and soluble fragments are released from the nanogels and into medium, which lead to an increased baseline fluorescence (Figure S4B, Supporting Information). Intense fluorescence peaks are still observed at roughly the same frequency, which is probably because nanogels were only partly degraded, so that they still remain fluorescent. The total amount of soluble degradation products was obtained from the baseline fluorescence of fully degraded nanogels incubated under accelerated conditions (pH 9, 37 °C, 6 h). Figure S4C (Supporting Information) shows that under these conditions the nanogels indeed completely degraded since no large fluctuations (pointing to the presence of nanoparticles) in the fluorescence signal were detected. The degree of degradation of nanogels incubated in plasma at 37 °C for 1, 3, 6, and 24 h was calculated by comparing the baseline fluorescence of samples to the total amount of fluorescence (Equation (6)).

The kinetics of degradation of nanogels in PBS and plasma at 37 °C is presented in Figure 5B. This figure shows that round 30–40% of labeled polymer was present in the medium after 3 h incubation in the form of soluble fragments, and the amount of soluble products subsequently increased slowly in time reaching about 60% soluble product after 24 h incubation. Figure 5B also shows that that no significant difference of degradation behavior can be observed in the two media. These results indicate that the degradation of the nanogels is a chemical process in which proteins and enzymes present in plasma have little contribution.

4. Conclusions

Three techniques were used and optimized to investigate the degradation behavior of nanogels differing in extent of PEGylation and crosslink density. fSPT results demonstrate that this is an attractive technique to assess the colloidal stability of the nanogels in biofluids (i.e., human plasma). TFF is able to reveal differences in degradation and filtration of nanogels with different degradation behaviors as an artificial in vitro circulation and filtration system. Furthermore, degradation of nanocarriers under biological conditions can be characterized directly in

vitro with FFS, which is likely predictive for in vivo behavior. All together, these advanced in vitro methods provide extra and valuable information on properties of nanocarriers, and can help identify and optimize nanocarrier-based drug products with desired in vivo behavior prior to animal studies.

Supporting Information

Supporting Information is available from the Wiley Online Library or from the author.

Acknowledgements

This research was partially supported by the China Scholarship Council.

Conflict of Interest

The authors declare no conflict of interest.

Keywords

degradation, fluorescence correlation spectroscopy (FFS), fluorescence single particle tracking (fSPT), stability, tangential flow filtration (TFF)

Received: April 2, 2017
Revised: May 20, 2017
Published online: November 20, 2017

[1] L. Bregoli, D. Movia, J. D. Gavigan-Imedio, J. Lysaght, J. Reynolds, A. Prina-Mello, *Nanomed.: Nanotechnol., Biol. Med.* **2016**, *12*, 81.
[2] A. Wicki, D. Witzigmann, V. Balasubramanian, J. Huwyler, *J. Controlled Release* **2015**, *200*, 138.
[3] T. L. Doane, C. Burda, *Chem. Soc. Rev.* **2012**, *41*, 2885.
[4] T. Lammers, V. Subr, K. Ulbrich, W. E. Hennink, G. Storm, F. Kiessling, *Nano Today* **2010**, *5*, 197.
[5] E. J. Cho, H. Holback, K. C. Liu, S. A. Abouelmagd, J. Park, Y. Yeo, *Mol. Pharmaceutics* **2013**, *10*, 2093.
[6] A. E. Nel, L. Madler, D. Velegol, T. Xia, E. M. V. Hoek, P. Somasundaran, F. Klaessig, V. Castranova, M. Thompson, *Nat. Mater.* **2009**, *8*, 543.
[7] H. Koide, T. Asai, K. Hatanaka, T. Urakami, T. Ishii, E. Kenjo, M. Nishihara, M. Yokoyama, T. Ishida, H. Kiwada, N. Oku, *Int. J. Pharm.* **2008**, *362*, 197.
[8] H. Gao, Q. He, *Expert Opin. Drug Delivery* **2014**, *11*, 409.
[9] A. Kolate, D. Baradia, S. Patil, I. Vhora, G. Kore, A. Misra, *J. Controlled Release* **2014**, *192*, 67.
[10] J. S. Suk, Q. Xu, N. Kim, J. Hanes, L. M. Ensign, *Adv. Drug Delivery Rev.* **2016**, *99*, 28.
[11] R. Gref, M. Lück, P. Quellec, M. Marchand, E. Dellacherie, S. Harnisch, T. Blunk, R. H. Müller, *Colloids Surf., B* **2000**, *18*, 301.
[12] D. E. Owens Iii, N. A. Peppas, *Int. J. Pharm.* **2006**, *307*, 93.
[13] J.-M. Rabanel, P. Hildgen, X. Banquy, *J. Controlled Release* **2014**, *185*, 71.
[14] A. Mokhtarzadeh, A. Alibakhshi, M. Hashemi, M. Hejazi, V. Hosseini, M. de la Guardia, M. Ramezani, *J. Controlled Release* **2017**, *245*, 116.
[15] V. D. Prajapati, G. K. Jani, J. R. Kapadia, *Expert Opin. Drug Delivery* **2015**, *12*, 1283.
[16] Q. Liu, C. Cai, C.-M. Dong, *J. Biomed. Mater. Res., Part A* **2009**, *88A*, 990.
[17] N. Samadi, C. F. van Nostrum, T. Vermonden, M. Amidi, W. E. Hennink, *Biomacromolecules* **2013**, *14*, 1044.
[18] S. Scheler, M. Kitzan, A. Fahr, *Int. J. Pharm.* **2011**, *403*, 207.
[19] Y. Chen, M. J. van Steenbergen, D. Li, J. B. van de Dikkenberg, T. Lammers, C. F. van Nostrum, J. M. Metselaar, W. E. Hennink, *Macromol. Biosci.* **2016**, *16*, 1122.
[20] R. Zhang, K. Luo, J. Yang, M. Sima, Y. Sun, M. M. Janát-Amsbury, J. Kopeček, *J. Controlled Release* **2013**, *166*, 66.
[21] P. Chytil, T. Etrych, L. Kostka, K. Ulbrich, *Macromol. Chem. Phys.* **2012**, *213*, 858.
[22] A. Sharma, T. Garg, A. Aman, K. Panchal, R. Sharma, S. Kumar, T. Markandeywar, *Artif. Cells Nanomed. Biotechnol.* **2016**, *44*, 165.
[23] A. J. Sivaram, P. Rajitha, S. Maya, R. Jayakumar, M. Sabitha, *Wiley Interdiscip. Rev.: Nanomed. Nanobiotechnol.* **2015**, *7*, 509.
[24] W. N. E. van Dijk-Wolthuls, S. K. Y. Tsang, J. J. Kettenes-van den Bosch, W. E. Hennink, *Polymer* **1997**, *38*, 6235.
[25] J. A. Cadée, M. De Kerf, C. J. De Groot, W. Den Otter, W. E. Hennink, *Polymer* **1999**, *40*, 6877.
[26] Y. Chen, O. Tezcan, D. Li, N. Beztsinna, B. Lou, T. Etrych, K. Ulbrich, J. M. Mestselaar, T. Lammers, W. E. Hennink, *Nanoscale* **2017**, *9*, 10404.
[27] K. Raemdonck, B. Naeye, K. Buyens, R. E. Vandenbroucke, A. Høgset, J. Demeester, S. C. De Smedt, *Adv. Funct. Mater.* **2009**, *19*, 1406.
[28] K. Braeckmans, K. Buyens, W. Bouquet, C. Vervaet, P. Joye, F. D. Vos, L. Plawinski, L. Doeuvre, E. Angles-Cano, N. N. Sanders, J. Demeester, S. C. D. Smedt, *Nano Lett.* **2010**, *10*, 4435.
[29] K. Buyens, B. Lucas, K. Raemdonck, K. Braeckmans, J. Vercammen, J. Hendrix, Y. Engelborghs, S. C. De Smedt, N. N. Sanders, *J. Controlled Release* **2008**, *126*, 67.
[30] L. Novo, K. M. Takeda, T. Petteta, G. R. Dakwar, J. B. van den Dikkenberg, K. Remaut, K. Braeckmans, C. F. van Nostrum, E. Mastrobattista, W. E. Hennink, *Mol. Pharmaceutics* **2015**, *12*, 150.
[31] T. Etrych, V. Šubr, J. Strohalm, M. Šírová, B. Říhová, K. Ulbrich, *J. Controlled Release* **2012**, *164*, 346.
[32] J. Kopeček, P. Kopečková, T. Minko, Z.-R. Lu, *Eur. J. Pharm. Biopharm.* **2000**, *50*, 61.
[33] J. Dommerholt, S. Schmidt, R. Temming, L. J. A. Hendriks, F. P. J. T. Rutjes, J. C. M. van Hest, D. J. Lefeber, P. Friedl, F. L. van Delft, *Angew. Chem., Int. Ed.* **2010**, *49*, 9422.
[34] R. Pola, A. Braunova, R. Laga, M. Pechar, K. Ulbrich, *Polym. Chem.* **2014**, *5*, 1340.
[35] Y. Jiang, J. Chen, C. Deng, E. J. Suuronen, Z. Zhong, *Biomaterials* **2014**, *35*, 4969.
[36] G. Zhang, Z. Yang, W. Lu, R. Zhang, Q. Huang, M. Tian, L. Li, D. Liang, C. Li, *Biomaterials* **2009**, *30*, 1928.
[37] G. R. Dakwar, K. Braeckmans, W. Ceelen, S. C. De Smedt, K. Remaut, *Drug Delivery Transl. Res.* **2017**, *7*, 241.
[38] B. J. Crielaard, A. Yousefi, J. P. Schillemans, C. Vermehren, K. Buyens, K. Braeckmans, T. Lammers, G. Storm, *J. Controlled Release* **2011**, *156*, 307.
[39] J. Lazarovits, Y. Y. Chen, E. A. Sykes, W. C. W. Chan, *Chem. Commun.* **2015**, *51*, 2756.
[40] P. Aggarwal, J. B. Hall, C. B. McLeland, M. A. Dobrovolskaia, S. E. McNeil, *Adv. Drug Delivery Rev.* **2009**, *61*, 428.
[41] W. N. E. van Dijk-Wolthuis, J. A. M. Hoogeboom, M. J. van Steenbergen, S. K. Y. Tsang, W. E. Hennink, *Macromolecules* **1997**, *30*, 4639.
[42] L. W. Seymour, R. Duncan, J. Strohalm, J. Kopeček, *J. Biomed. Mater. Res.* **1987**, *21*, 1341.
[43] C. S. Genovesi, *PDA J. Pharm. Sci. Technol.* **1983**, *37*, 81.

[44] G. Dalwadi, H. A. E. Benson, Y. Chen, *Pharm. Res.* **2005**, *22*, 2152.
[45] G. Dalwadi, B. Sunderland, *Drug Dev. Ind. Pharm.* **2008**, *34*, 1331.
[46] C. B. Anders, J. D. Baker, A. C. Stahler, A. J. Williams, J. N. Sisco, J. C. Trefry, D. P. Wooley, I. E. Pavel Sizemore, *J. Visualized Exp.* **2012**, 4167.
[47] J. Zaloga, M. Stapf, J. Nowak, M. Pöttler, R. P. Friedrich, R. Tietze, S. Lyer, G. Lee, S. Odenbach, I. Hilger, C. Alexiou, *Int. J. Mol. Sci.* **2015**, *16*, 19291.
[48] M. Longmire, P. L. Choyke, H. Kobayashi, *Nanomedicine* **2008**, *3*, 703.
[49] T. Matsubara, H. Abe, H. Arai, K. Nagai, A. Mima, H. Kanamori, E. Sumi, T. Takahashi, M. Matsuura, N. Iehara, A. Fukatsu, T. Kita, T. Doi, *Lab. Invest.* **2006**, *86*, 357.
[50] J. F. Bertram, M. C. Soosaipillai, S. D. Ricardo, G. B. Ryan, *Cell Tissue Res.* **1992**, *270*, 37.
[51] H. B. Lee, M. D. Blaufox, *J. Nucl. Med.* **1985**, *26*, 72.
[52] T. Sakaeda, K. Fukumura, K. Takahashi, S. Matsumura, E. Matsuura, K. Hirano, *J. Drug Targeting* **1998**, *6*, 261.
[53] P. Chytil, M. Sirova, E. Koziolova, K. Ulbrich, B. Rihova, T. Etrych, *Phys. Res.* **2015**, *64*, S41.
[54] Y. Noguchi, J. Wu, R. Duncan, J. Strohalm, K. Ulbrich, T. Akaike, H. Maeda, *Jpn. J. Cancer Res.* **1998**, *89*, 307.
[55] C. D. Hein, X. Liu, D. Wang, *Pharm. Res.* **2008**, *25*, 2216.
[56] H. C. Kolb, K. B. Sharpless, *Drug Discovery Today* **2003**, *8*, 1128.